International Journal of GEOMATE, Sept., 2022, Vol.23, Issue 97, pp.38-44
ISSN: 2186-2982 (P), 2186-2990 (O), Japan, DOI: https://doi.org/10.21660/2022.97.1765
Geotechnique, Construction Materials and Environment

INVESTIGATION OF TUNNEL RESPONSE DUE TO THE EFFECT OF ADJACENT LOADED PILE ROW BY 3D SIMULATION ANALYSIS

Narunat Heama[1], and *Prateep Lueprasert[1]

[1]Department of Civil Engineering, School of Engineering, King Mongkut's Institute of Technology Ladkrabang, Bangkok, Thailand

*Corresponding Author, Received: 16 Feb. 2022, Revised: 07 June 2022, Accepted: 02 Aug. 2022

ABSTRACT: The construction of tunnels for transportation, wastewater, electricity, etc., in the major cities has flourished. In the meantime, other infrastructures such as elevated trains, and flyovers, are continually constructed for urbanization. Under a soft ground condition, they are supported by the pile foundations required pile rows which are possibly located along the existing tunnel. A common challenge encountered in the loaded pile row of the new adjacent structures is inevitably inducing soil stress changes and deformation of existing tunnels. Thus, an assessment of the impact of pile underloading on the integrity of the existing tunnels is essential. The three-dimensional finite element analyses (3D FEA) with two pile conditions were carried out. The tunnel responses (transversal deformation and additional forces) at different transverse sections are presented. The maximum response of those was shown in the monitoring section (center of pile row section). Meanwhile, the torsion deformations are maximum as the 12 – 30 m ($\approx 1.5D_{tunnel}$ - $4.5D_{tunnel}$) away from the center of the pile row. For both short and long pile conditions, the influence zones of loaded pile row in a longitudinal direction are independent of the pile length and extended horizontal distance of $2D_{tunnel}$ away from the last pile within a row.

Keywords: Transversal deformation, Torsional deformation, Tunnel response, 3D finite element analysis

1. INTRODUCTION

The construction of tunnels for transportation, wastewater, electricity, communication cables, etc., is flourishing around the major cities in the world and has become a focus of urban infrastructure development. In the meantime, other infrastructures such as elevated trains, flyovers, and crossing bridges, are continually constructed for urbanization. Under soft ground conditions, they are supported by the pile foundations. A common challenge encountered is that the loaded piles of the new adjacent structures are inevitably close to the existing tunnels. Typically, the displacement of soil generated by pile settlement (under loading) induces additional deformation and change in structural forces to an existing adjacent tunnel. Such changes may lead to extremely negative effects on the integrity and serviceability of the tunnels. Thus, an assessment of tunnel response due to the impact of piles under loading is crucial.

Numerical analysis has become an increasingly popular and powerful analytical tool for modeling. A three-dimensional finite element analysis (3D-FEA) is often used to study tunneling works [1]-[5]. In analyses of existing tunnel response due to new construction (i.e., deep excavation, tunneling), the internal forces, deformation monitored at different transverse sections and the torsion behavior are determined [6], [7].

During the past few decades, many investigations of the influence of loaded piles on adjacent or underlying existing tunnels have been concerned. The parameters of adjacent loaded piles (i.e., pile diameter, pile length, pile spacing, and the number of piles) were considered only to evaluate the tunnel transversal deformation and structural forces in tunnel lining in a soft soil profile. The analysis results suggest the mechanisms behind tunnel-soil-pile interaction and safe clearance between the tunnel and pile or pile row [8]-[10]. However, the tunnel responses due to adjacent loaded piles were presented in only one transverse section at the monitoring section or center of the model. Their results at different transverse sections and torsional deformation have been neglected.

Specifically, this research focuses on the effect of adjacent loaded pile rows on the existing tunnel. The simulations were carried out by 3D finite element (FE) models. There were two simulation models: 3D FE full models with short pile row and long pile row. For the pile row, there were simulated embedded piles. The existing tunnel responses (e.g., the lining deformation and additional structural forces) are presented and discussed. Typically, the torsion behavior of the existing tunnel after pile row under loading is highlighted.

Table 1 Parameters for soil layer of 3D and 2D simulation models.

Layer	1	2	3	4	5	6	7	8
Soil type	Made Ground	Soft Clay	Medium Clay	1st Stiff Clay	1st Clayey Sand	2nd Stiff Clay	Hard Clay	2nd Clayey Sand
γ_{soil} (kN/m^3)	18	16.5	17.5	19.5	19	20	20	20
c' (kPa)	1	5	15	25	0	30	40	0
$\emptyset'$ (°)	25	27	27	28	33	28	28	36
Ψ' (°)	0	0	0	0	5	0	0	5
E_{oed}^{ref} (MPa)	45.6	5	20	60	80	60	60	80
E_{50}^{ref} (MPa)	45.6	5	20	60	80	60	60	80
E_{ur}^{ref} (MPa)	136.8	15	100	180	240	180	180	240
ν_{ur}	0.2	0.2	0.2	0.2	0.2	0.2	0.2	0.2
m	1	1	1	1	0.5	1	1	0.5
K_0^{nc}	0.58	0.6	0.6	0.5	0.55	0.5	0.5	0.5
R_f	0.9	0.9	0.9	0.9	0.9	0.9	0.9	0.9
G_{max} (MPa)	-	15	45	80	200	80	130	240
$\gamma_{0.7}$	-	0.08	0.11	0.12	0.014	0.12	0.15	0.02
Analysis type	Drained	Undrained	Undrained	Undrained	Undrained	Undrained	Undrained	Undrained

Table 2 Material properties of the 3D and 2D FE simulation models.

	Young's modulus (E, kN/m^2)	Poisson's ratio (ν)	Unit weight (γ, kN/m^3)
Tunnel lining	31 x 10^6	0.20	24
Loaded pile	31 x 10^6	0.20	24
EPB shield	210 x 10^6	0.28	78
Grouting layer	1 x 10^6	0.30	21

2. FINITE ELEMENT SIMULATION

The continuous tunnel lining and embedded pile row were modeled by Plaxis 3D software version 2018. In engineering practice, the tunnel is constructed by segmental lining. However, in the case of the tunnel where the location is shallow, the modeling of continuous lining is sufficient for consideration of the structural forces in tunnel lining [11]. The pile row was modeled by an embedded pile row which can reduce the complexity of a high number of pile models [12]. The wished-in-place bored pile is modeled on one side of the tunnel. Before applying the pile loading, the displacements are reset to zero. The working load is 40% of the ultimate pile capacity determined by the α-method [13]. The pile row consisted of 13 piles to eliminate the edge effect [14].

2.1 Characteristics of Model

In Fig. 1, the lining thickness, T, of 0.3 m, outer diameter, D_{tunnel}, of 6.3 m, and the center of the tunnel below the ground surface, Z_{tunnel}, of 20.5 m are fixed throughout this study. The diameter of the bore pile, D_{pile}, of 1.0 m, and clearance, C, of 0.5 m are also fixed. The pile spacing was varied, S, of $2D_{pile}$, $3D_{pile}$, $4D_{pile}$, and $6D_{pile}$, positions of pile tips, Z_{pile}, are at the 17.35 m and 57.0 m below the ground surface, representing the short pile and long pile conditions for determining the existing tunnel response, respectively.

The soil profile at Sukhumvit station, one of the MRTA Blue Line Project's stations (section CS-8C of the project), was chosen to simulate and analyze in the study. Figure 2 depicts the geological conditions, which include (1) Made Ground or fill material at 0–2.5 m, (2) Soft Clays at 2.5–12 m, (3) Medium Clays at 12–14 m, (4) 1st Stiff Clays at 14–20 m, (5) A thin seam of 1st Clayey Sand is found at 20-21.5 m, (6) 2nd Stiff Clays at 21.5-26.5 m, (7) Hard Clays at 26.5-54 m, and (8) 2nd Clayey Sand at 54–80 m. The groundwater condition is piezometric drawdown due to the overpumping of the groundwater in the past, as shown in Fig. 2.

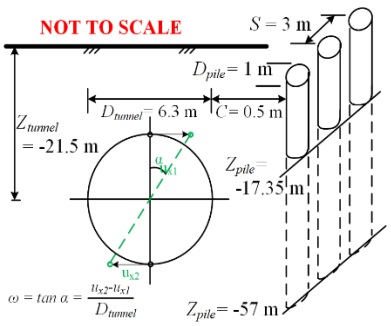

Fig. 1 Geometric parameters in the modeling

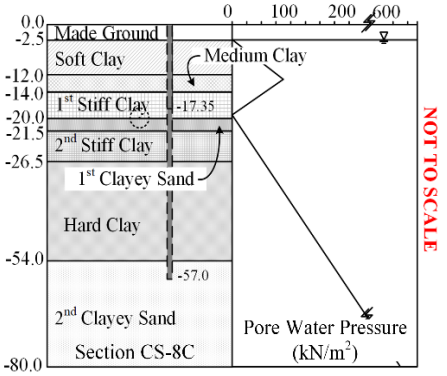

Fig. 2 Soil profile and pore water pressure

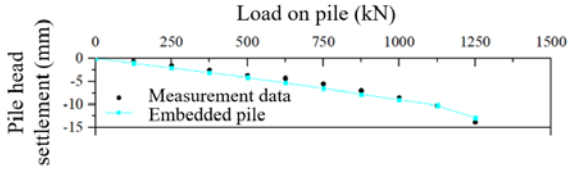

Fig. 3 Loaded single pile simulation

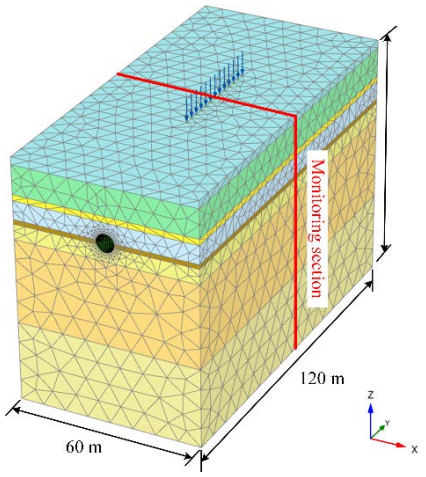

Fig. 4 Boundary and FE mesh

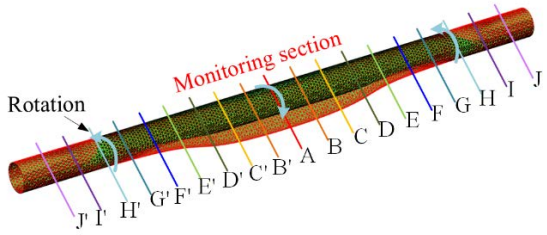

Fig. 5 Details of the monitoring sections along tunnel lining

2.2 Model Properties

In the 3D simulation models, the hardening soil model with small-strain stiffness (HSS) was adopted to model all layers of soils except the Made Ground Layer, which is modeled by the Hardening Soil model (HSM). Table 1 presents the parameters of the soil profile of the capital Bangkok. The properties of the Bangkok subsoil were adopted from a previous study [15], [16]. The tunnel lining, EPB shield, grouting layer, and bored pile were modeled as a linear elastic material. The material parameters listed in Table 2 were used in the study. The interface friction value (R_{inter}) between the structural elements (EPB, tunnel lining, or bored piles), and the surrounding soil was chosen to be 0.9 as suggested in previous research [9], [17].

The soil layer and grouting layer were discretized into the volume elements or the 10-node tetrahedral elements. The 6-node triangular plate element was used to model the tunnel lining and EPB shield. The embedded pile consists of beam elements which can be 3-node line elements. For the embedded pile, the input parameters consist of diameter (D), the unit weight (γ), and young's modulus (E). In the model, the unit weight of the embedded pile ($\gamma_{embedded}$) was subtracted by the unit weight of soil (subsoilγ_{soil}) [12].

2.3 Model Validation

The static pile load test of a 23-story residential complex at or near the CS-8C section (It is located approximately 500 m away) was used to validate against the computed single-pile head settlements from the FE model.

Figure 3 shows comparing between the static pile load test and simulated pile head settlements, given the pile diameter of 1 m and pile length of 57.0 m. The results were generally agreeable. This implies that the properties of soil and pile are reasonable to subsequently evaluate the effect on the existing tunnel due to the adjacent loaded pile row for this study. Note that the simulation of 17.35 m pile length (short pile) was not compared due to the unavailability of field static pile load test data of the short pile.

2.4 3D Simulation Model

From a previous study, the sufficient boundary of the 3D numerical model with TBM tunneling suggested by Mroueh and Shahrour [18] was the advancement of 4.0D_{tunnel} behind and ahead of the face of tunnel excavation and lateral distance from the edge of the tunnel of 3.5D_{tunnel}. Thus, the lateral distance from a tunnel edge of 4.25D_{tunnel}, and the advancement of 5.5D_{tunnel} behind and ahead of the monitoring section in this study, as shown in Fig. 4, are enough to fully model the 3D tunneling problem.

On the lateral boundaries of the 3D model, the lateral displacements in the x- and y-directions were fixed, while vertical displacement in the z-direction was permitted. The horizontal and vertical displacements were both fixed at the bottom boundary. For a good level of accuracy result, finer meshes are generated in the zone around the tunnel and pile. The total number of elements was approximately 260,000, and the total number of nodes was approximately 320,000. The loaded pile row was located on one side of the existing tunnel.

3. SIMULATION RESULTS AND DISCUSSION

3.1 Transversal Deformation

In this study, the tunnel deformations in the transverse direction were investigated along the longitudinal direction of the existing tunnel as shown in Fig. 5. This figure presents the tunnel deformation in the transverse direction with 6 m of horizontal distance between cross- sections. The reference of tunnel lining is represented by a bold line, the circumferential deformation along a longitudinal direction with a magnification ratio of 1:1000. Note that the deformation after tunneling is excluded.

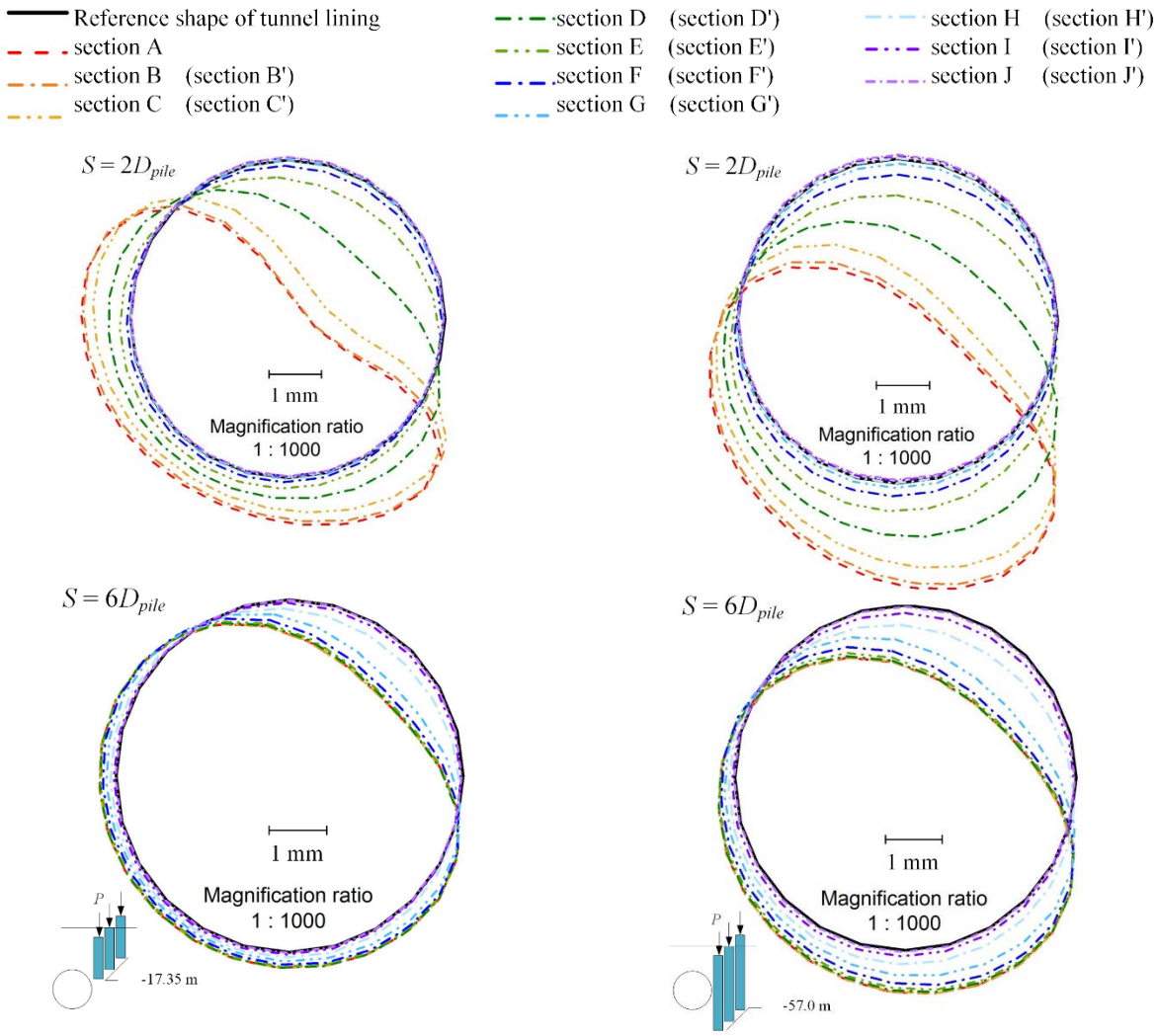

(a) Pile length of 17.35 m (short pile) (b) Pile length of 57.0 m (long pile)

Fig. 6 Simulated tunnel deformation as a result of adjacent loaded pile row, given $S = 2D_{pile}$ and $6D_{pile}$

Figure 6 illustrates the circumferential deformation at the different transverse sections along the tunnel axis, given $S = 2D_{pile}$ and $6D_{pile}$. The monitoring section was located in section A (the center of the models). Section A to J' and section A to J are symmetry. It can be seen that in both cases of short and long pile conditions, given $S = 2D_{pile}$ and $3D_{pile}$, the lining at section D' to D distorts into a kidney or ellipse shape inclined to the side closer to the pile. The tunnel deformation slightly changes at sections E' to J' and sections E to J. It is attributed to the different degrees of adjacent loaded pile row effect. For cases of $S = 4D_{pile}$ and $6D_{pile}$, the tunnel lining distorts into a kidney or ellipse shape at section E' to E and section G' to G, respectively. With the distance considered from the monitoring section (section A), the transversal deformations of the tunnel lining decrease with increasing distance and pile spacing.

Considering the pile conditions, the effect of a long pile row is larger than a short pile row. This is similar to the previous study [9]. However, it is worth noting that, with the dual influences of adjacent loaded pile row in both short and long pile cases, the tunnel deformation slightly changes at the section D'-D when $S = 2D_{pile}$ and $3D_{pile}$ and section E' to E and section G' to G when $S = 4D_{pile}$ and $6D_{pile}$, respectively. The pile length may not affect circumferential deformation at the different transverse sections along the tunnel axis.

3.2 Additional Forces in Tunnel Lining

Figure 7 illustrates the simulated additional bending moment (ΔM) and axial force (ΔN) in circumferential direction due to adjacent loaded pile row with short pile condition, given $S = 2D_{pile}$ and $6D_{pile}$. The tunnel crown is an origin ($\theta = 0^{o}$). In the figures, the ΔM and ΔN were obtained at different cross-sections (section A to section J) as the same section assigned to monitoring the tunnel deformation.

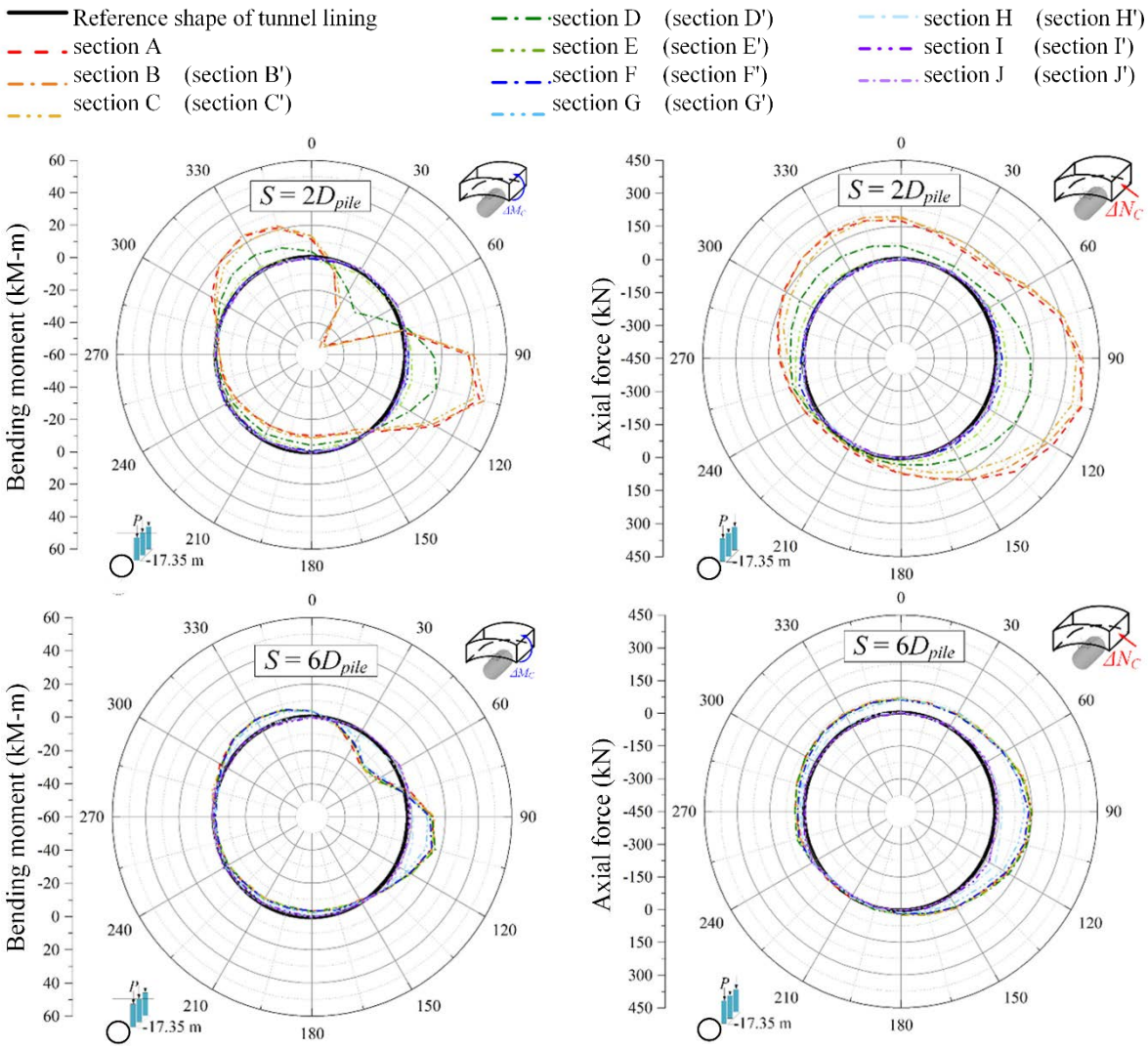

(a) Pile length of 17.35 m (short pile) (b) Pile length of 57.0 m (long pile)

Fig. 7 Additional lining forces circumferential direction with short pile condition given $S = 2D_{pile}$ and $6D_{pile}$

The calculation of the additional bending moment and axial force is shown in Eq**.** (1) and (2)**.** When M_1 and N_2 are structural forces in tunnel lining before pile loading, M_2 and N_2 are structural forces after pile loading. In this research, a positive value of ΔM and **represents** an increasing value, whereas a negative value represents a decreasing value.

$$\Delta M = M_2 - M_1 \quad (1)$$

$$\Delta N = N_2 - N_1 \quad (2)$$

The ΔM increased in the range of $\theta = 285^o$ to 0^o and 70^o to 140^o and decreased in the range of $\theta = 0^o$ to 70^o and 140^o to 285^o for both short and long piles, as shown in Fig. 7(a). The maximum positive and negative ΔM were at θ of approximately 105^o and 45^o for the short pile and approximately 120^o and 45^o for the long pile. By comparison, the ΔM under the short pile condition was more pronounced than under the long pile condition. It is seen from the figure that the simulated ΔM was is inversely correlated to the pile spacing and longitudinal distance for both short and long piles.

Figure 7(b) illustrates the in the circumferential direction, given a pile length of 17.35 m. The only increases with a maximum value at θ of approximately 105^o for both short and long piles. For comparison, both short and long pile conditions are similar ΔM . Their results closely resembled the tunnel deformation in the longitudinal direction. This supports that the effect on the existing tunnel in a longitudinal direction may not depend on pile length.

3.2 Torsion Behavior

Figure 8 shows the distribution of rotation indexed by ω of the existing tunnel along the tunnel axis due to nearby loaded pile rows in both short and long pile conditions. To identify the rotation behavior of the tunnel, a qualitative evaluation method is proposed as follows [6]:

$$\omega = \tan\alpha = \frac{u_{x2} - u_{x1}}{D_{tunnel}} \quad (3)$$

where ω is the rotation index, α is the rotation angle of the tunnel, D_{tunnel} is the diameter of the tunnel, u_{x1} and u_{x2} are the horizontal displacement of the crown and invert of the tunnel, respectively (see Fig. 1).

The ω is assumed to be positive when the tunnel rotates anticlockwise and negative when it rotates clockwise. In short pile condition, the tunnel rotates anticlockwise at the monitoring section (section A). The ω gradually decreases in the range of 6 – 30 m, 12 – 30, 18 – 36 m and 30 – 48 m with pile spacing S = $2D_{pile}$, $3D_{pile}$, $4D_{pile,}$ and $6D_{pile}$, respectively, as shown in Fig. 8(a).

In long pile conditions, the tunnel rotates anticlockwise in the range of 0 – 18 m, 0 – 24, 0 – 30 m, and 0 – 42 m with pile spacing S = $2D_{pile}$, $3D_{pile}$, $4D_{pile,}$ and $6D_{pile}$, respectively. Then the tunnel gradually turned from anticlockwise rotation to clockwise rotation with an increase in the horizontal distance, as illustrated in Fig. 8(a). In this research, the rotation of the existing tunnels caused by the nearby loaded pile ranges from 0.16×10^{-4} to -0.00×10^{-4} and 0.05×10^{-4} to -0.03×10^{-4} for short pile and long pile conditions, respectively. These results reveal that the maximum or minimum of ω is not located in the monitoring section. In both cases, the ω was inversely correlated to the pile spacing while the ω remained unchanged at a horizontal distance of 24, 30, 36 and 48 m away from the monitoring section with pile spacing S = $2D_{pile}$, $3D_{pile}$, $4D_{pile}$ and $6D_{pile}$, respectively.

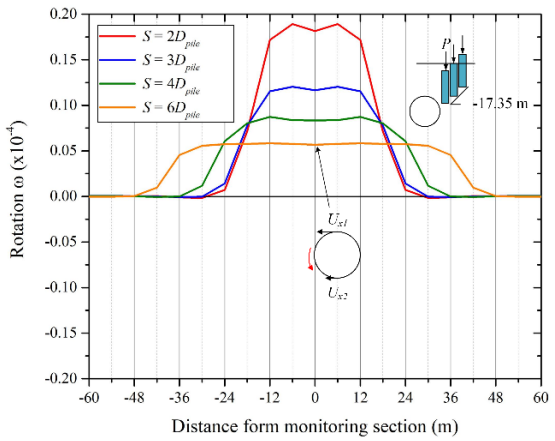

(a) pile length of 17.35 m

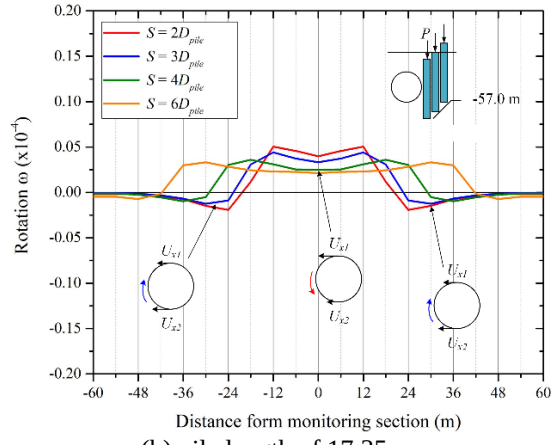

(b) pile length of 17.35 m

Fig. 8 Rotation of existing tunnel due to adjacent loaded pile row

In some tunnel works, structural forces in tunnel lining are the main concern, and torsional deformation may be neglected [19]. However, the ω due to adjacent loaded pile row may also experience large torsional deformation, which may lead to track distortion and even poses a risk to the safe operation of the train. Therefore, regarding the effect of adjacent loaded pile row on the existing tunnel, be not only careful of the structural forces in tunnel lining but also the torsional deformation of the tunnel should be a concern.

5. CONCLUSIONS

This study investigated the effect on existing tunnels due to adjacent loaded pile rows in terms of tunnel deformation, torsional deformation, and additional lining force (bending moment and axial force). The simulations were carried out by Plaxis 3D software, with 13 piles within the row. The simulation results were discussed. The pile diameter was 1 m, and the pile lengths were 17.35 m (short pile) and 57.0 m (long pile), respectively. The pile spacing (S) was varied at $2D_{pile}$, $3D_{pile}$, $4D_{pile}$, $6D_{pile}$. The edge-to-edge clearance (C) was fixed at 0.5 m. The conclusions are as follows:

1. The adjacent loaded pile row leads to tunnel responses (deformation and variation of internal forces) in the transverse direction accordingly. The tunnel deformation and additional forces (bending moment and axial force) become significant at the center of the pile row. Meanwhile, the torsion deformations are maximum as the 12 – 30 m (≈ $1.5D_{tunnel}$ - $4.5D_{tunnel}$) away from the center of the pile row.
2. The influence of the adjacent loaded pile row on the existing tunnel in the longitudinal direction is extended the horizontal distance of the $2D_{tunnel}$ away from the last pile within the row.
3. The unrecoverable torsional deformation of the tunnel was induced by a loaded pile row, which is distinct from the perpendicular case. For both short and long pile conditions, the tunnel gradually rotates in a range of 0 – 36 m. (≈ $0D_{tunnel}$ - $6D_{tunnel}$).
4. The influence zones of the loaded pile row in the longitudinal direction are independent of the pile length.

In this study, the pile diameter (D_{pile}) and clearance (C) were fixed, and tunnel lining was simulated based on the

continuous lining. Future work considering the effects of joints and varying D_{pile} and C should be done to extend the scope of the study.

ACKNOWLEDGMENTS

The authors wish to express their thankfulness to the Faculty of Engineering, King Mongkut's Institute of Technology Ladkrabang and TRF Basic Research for the financial support through Grant KREF016317 and Contract PHD60I0032.

REFERENCES

[1] Dang V. K., Dias D., Do N. A., and Vo T. H., Impact of blasting at tunnel face on an existing adjacent tunnel, International Journal of GEOMATE, Vol. 15, Issue 47, 2018, pp.22-37.

[2] Shiau J. and Sams M., Estimation of tunneling induced ground settlement using pressure relaxation method, International Journal of GEOMATE, Vol. 13, Issue 39, 2017, pp.132-139.

[3] Chaiyasarn K., Sharma M., Ali L., Khan W., and Poovarodom N., Crack detection in historical structures based on convolutional neural network, International Journal of GEOMATE, Vol. 15, Issue 51, 2018, pp.240-251.

[4] Lueprasert P., Jonpradist P., and Suwansawat S., Tunneling simulation in the soft ground using shell elements and grouting layer, International Journal of GEOMATE, Vol. 12, Issue 31, 2017, pp.51-57.

[5] Zheng G., Pan J., Li Y., Cheng X., Tan F., Du Y., and Li, X. (2020), Deformation and Protection of Existing Tunnels at an Oblique Intersection Angle to an Excavation", International Journal of Geomechanics, 20, 2020.

[6] Lin X. T., Chen R. P., Wu H. N., and Cheng H. Z., Deformation behaviors of existing tunnels caused by shield tunneling undercrossing with oblique angle, Tunnelling Underground Space Technol. 89, 2019, pp.78–90.

[7] Zheng G., Pan J., Li Y., Cheng X., and Li X., Deformation and protection of existing tunnels at an oblique intersection angle to an excavation, International Journal of Geomechanics, Vol. 20, No. 8, 2020.

[8] Heama N., Jongpradist P., Lueprasert P., and Suwansawat S., Investigation on tunnel responses due to adjacent loaded pile by 3D finite element analysis, International Journal of GEOMATE, Vol. 12, Issue 31, 2017, pp.63-70.

[9] Lueprasert P., Jongpradist P., Jongpradist P., and Suwansawat S., Numerical investigation of tunnel deformation due to adjacent loaded pile and pile-soil-tunnel interaction, Tunnelling and Underground Space Technology, 70, 2017, pp.166-181.

[10] Nematollahi M. and Dias D., Three-dimensional numerical simulation of pile-twin tunnels interaction – Case of the Shiraz subway line, Tunnelling and Underground Space Technology, 86, 2019, pp.75-88.

[11] Michael K., Dimitris L., Ioannis V., and Petros, F., Development of a 3D finite element model for shield EPB tunneling, Tunnelling, and Underground Space Technology, 65, 2017, pp.22-34.

[12] Tschuchnigg F. and Schweiger H. F. (2015), The embedded pile concept - Verification of an efficient tool for modeling complex deep foundations, Computers and Geotechnics, 63, 2015, pp.244–254.

[13] Skempton A. W., Cast In-Situ Bored Piles in London Clay, Géotechnique, 9, 1959, pp.153–173.

[14] Heama N., Jongpradist P., Lueprasert P., and Suwansawat S., Investigation on pile-soil-tunnel interaction due to adjacent loaded pile row by 3D FEM, The International Conference on Engineering, Applied Sciences and Technology (ICEAST), 192, 2018, pp.792-795.

[15] Likitlersuang S., Teachavorasinskun S., Surarak C., Oh E., and Balasubramaniam A., Small strain stiffness and stiffness degradation curve of Bangkok Clays, Soils and Foundations, 53, 2013, pp.498–509.

[16] Rukdeechuai T., Jongpradist P., Wonglert A., and Kaewsri T., Influence of Soil Models on Numerical Simulation of Geotechnical works in Bangkok subsoil, Journal of Research and Development, 20, 2009.

[17] Mathew G. V. and Lehane B. M., Numerical back-analyses of greenfield settlement during tunnel boring, Canadian Geotechnical Journal, 50, 2013, pp.145–152.

[18] Mroueh H. and Shahrour I., Three-dimensional finite element analysis of the interaction between tunneling and pile foundations, International Journal for Numerical and Analytical Methods in Geomechanics, 2002.

[19] Chen H. H., Li J. P., and Li L., Performance of a zoned excavation by bottom-up technique in Shanghai soft soils, Journal of Geotechnical and Geoenvironmental Engineering, Vol. 144, Issue)11(, 2018.